Processes **2014**, *2*, 141-157; doi:10.3390/pr2010141

OPEN ACCESS

processes

ISSN 2227-9717

www.mdpi.com/journal/processes

Article

Enhanced Performance of Oxidation of Rosalva (9-decen-1-ol) to Costenal (9-decenal) on Porous Silicon-Supported Silver Catalyst in a Microstructured Reactor

Enhong Cao [1], Ioannis Zuburtikudis [2,3], Noor Al-Rifai [1], Mark Roydhouse [1] and Asterios Gavriilidis [1,*]

[1] Department of Chemical Engineering, University College London, Torrington Place, London WC1E 7JE, UK; E-Mails: e.cao@ucl.ac.uk (E.C.); noor.al-rifai.10@ucl.ac.uk (N.A.-R.); mroydhouse@googlemail.com (M.R.)

[2] Department of Mechanical and Industrial Design Engineering, T.E.I. of Western Macedonia, Kozani 50100, Greece; E-Mail: Ioannis.z@uaeu.ac.ae

[3] Department of Chemical and Petroleum Engineering, United Arab Emirates University, Al Ain, P.O.Box: 15551, UAE

* Author to whom correspondence should be addressed; E-Mail: a.gavriilidis@ucl.ac.uk; Tel.: +44-(0)-20-7679-3811; Fax: +44-(0)-20-7383-2348.

Received: 24 November 2013; in revised form: 9 January 201□ Accepted: 16 January 201□ Published: 29 January 2014

Abstract: The use of metal-assisted HF chemical etching as a convenient technique to produce a few microns thick porous layer in silicon microchannels was demonstrated. Gas phase selective oxidation of rosalva to its aldehyde (costenal) was performed in glass/silicon microstructured reactors at temperatures of 375–475 °C on silver catalyst which was deposited on both porous and flat silicon surface by sputter-coating. The effects of temperature (375–475 °C), rosalva concentration (1.17%–3.43%), O_2 to rosalva ratio (0.5–20) and residence time on the reaction were investigated. The reactivity of rosalva on the porous silicon supported silver was 5.7–6.4 times higher than on the thin film silver catalyst at 450 °C. Furthermore, activation energy for the porous silicon supported silver was lower. Isothermal conditions in the microreactors allowed high conversion and selectivity to be achieved in a wide range of temperature and oxygen concentration. At typical reaction conditions (1.75% rosalva, O_2/rosalva = 3, residence time 18 ms and 450 °C), conversion of 97% and selectivity of 95% to costenal was achieved, corresponding to a turnover frequency of 268 h^{-1}.

Keywords: microreactor; porous silicon; oxidation; rosalva; silver catalyst

1. Introduction

Catalytic selective oxidation of alcohols is a fundamental process in synthetic chemistry as carbonyl compounds have widespread applications in the flavor, pharmaceutical, agrochemical, and fragrance industries [1,2]. Oxidation of alcohols by using air or molecular oxygen has been proposed as a green methodology to replace traditional stoichiometric inorganic oxidants such as K_2CrO_7 and $KMnO_4$, where the dispersal of unwanted by-products and the heavy metal waste represents a huge impact on the environment [3]. The oxidation of alcohols on metal catalyst with molecular oxygen can be performed in the liquid phase or in the gas phase, depending on the thermal stability and volatility of reagents and products. Gas phase oxidation of alcohols with air or oxygen represents an attractive route for the industrial production of carbonyl compounds, but successful industrial application rely on the catalyst to provide high reactivity and selectivity and the reactor design to prevent the degradation of reactants and products at high reaction temperature. Considerable research has been carried out on development of metals or supported metal catalysts for gas phase oxidation of a wide range of alcohols [4–9]. The gas phase oxidation for simple alcohols is well established on the industrial scale (e.g., methanol oxidation to formaldehyde on silver catalyst). In the BASF process for citral synthesis, isoprenol is converted to isoprenal on a supported silver catalyst at 500 °C with a residence time of about 0.001 s [10]. These examples show that such reactions can be carried out in catalytic reactors provided that very short residence time and fast quenching after reaction can be achieved.

The application of microreaction technology to catalytic oxidation reactions is proving to be beneficial due to the ability to circumvent problems such as high exothermicity and poor control of reaction conditions, commonly associated with catalytic oxidation reactions [11]. The large surface area to volume ratio inherent to microreactors allows even highly exothermic reactions to be performed isothermally, resulting in higher selectivity and minimum waste. The small inventories of catalyst and reactants in a microreactor result in a process requiring only a few milligrams of catalyst and allowing operation within the flammability limits. In our previous research, oxidative dehydrogenation of prenol (3-methyl-2-buten-1-ol) to the corresponding aldehyde was performed in a silicon-glass microreactor on silver catalyst with high selectivity [12]. The silver catalyst was incorporated into the reaction channel by sputtering deposition. In this way, the thin film can only provide limited surface area for catalytic reactions. To generate high surface area in thin films, various methods have been reported. These include sol-gel coating [13,14], anodic oxidation of silicon [15], and more recently, growing nanoparticles and nanosprings on surfaces [16]. With silicon-glass microstructured reactors, the formation of porous silicon in reaction channels is a convenient method to increase surface area. Porous silicon is an important material for the semiconductor industry [17]. It has various applications in chemical devices, such as a high surface area support for chemical and biological applications [18,19], as porous membrane for small fuel cells [20] and as a stationary phase in liquid chromatography chips [21,22]. Various methods have been developed to fabricate porous silicon structures such as reactive ion etching, electrochemical etching (anodic oxidation), and

metal-assisted chemical etching [23]. Among these methods, metal-assisted chemical etching provides a low temperature, simple and cost effective method for fabricating various silicon nano- and micro-structures in a controllable way over large areas [17,23,24].

Costenal (9-decenal) has an extremely powerful aldehydic olfactive note and is used in flavors and fine fragrances. It can be prepared from rosalva (9-decen-1-ol) via a Swern oxidation [25] or other liquid phase oxidation methods which involve many reaction steps and product purification processes [26–28]. Gas phase selective oxidation of rosalva could be a useful route for preparing the corresponding aldehyde but little investigative work has been done. Gallezot *et al.* [29] reported the gas phase oxidation of rosalva over Ag/SiC catalyst in a laboratory scale reactor at 450 °C. The highest costenal yield of 51% was obtained at conversion of 70% with a contact time of 28 ms. In this paper, we report the investigation of the gas phase rosalva oxidation on silver catalyst in microstructured reactors. Metal-assisted HF/H_2O_2 chemical etching was used to produce porous silicon in the microreactor channel where catalytic reaction takes place in order to increase the available surface area. Enhanced performance of the reaction on the porous silicon supported silver catalyst was demonstrated.

2. Experimental

2.1. Preparation of Microstructured Reactors

A silicon-glass microstructured reactor was prepared in four steps: Silicon etching, formation of porous silicon in the reaction channel, deposition of silver catalyst on the porous silicon and covering the silicon microreactor with a glass wafer through anodic bonding. A schematic illustration of the fabrication process is shown in Figure 1.

Figure 1. Schematic illustration of the microreactor fabrication process: (**a**) photolithography and deep reactive ion etching, (**b**) porous silicon formation and (**c**) catalyst deposition and glass bonding.

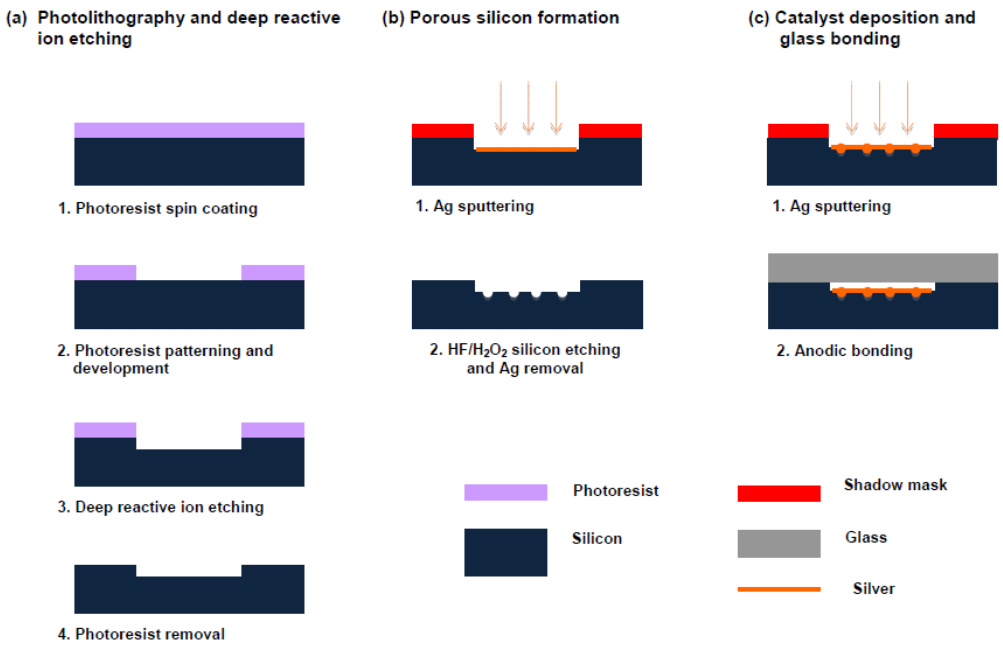

The microreactor, which contains a wide reaction channel (6 mm) with a channel depth of 0.12 mm, as shown in Figure 2a, was fabricated on a 4" silicon wafer (n<100>, 0–10 Ω cm, 0.525 mm thick) using photolithography and deep reactive ion etching (DRIE) (STS ASE; Oxford Instruments, Oxfordshire, UK). The procedure has been described elsewhere [30]. After DRIE, the wafer was diced using an automated precision dicing saw (Disco DADS 3230; Disco Corporation, Tokyo, Japan) and five microreactors were obtained from each 4" silicon wafer.

Figure 2. Microstructured reactor (**a**) without and (**b**) with silver catalyst and glass cover.

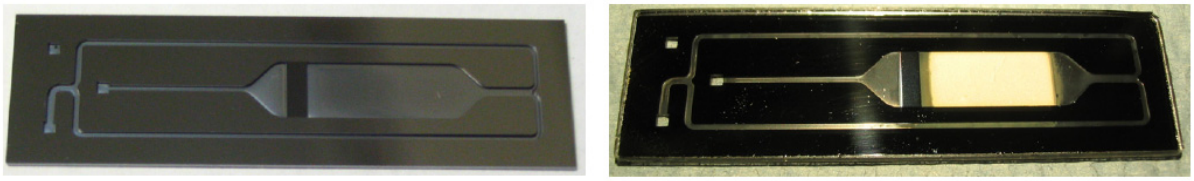

(a) **(b)**

2.1.1. Porous Silicon Formation

The porous silicon structures were formed in the reaction channel by a metal-assisted HF/H_2O_2 chemical etching process [23]. The microreactors were first cleaned using piranha solution (a mixture of 1:1 concentrated H_2SO_4 to 30% H_2O_2) for 20 min. To define the porous silicon area in the reaction channel, a shadow mask with a window of 6 mm × 12 mm was aligned to the microreactor. A thin layer of silver (4–5 nm) was then deposited in this window using a sputter coater (K675XD; Emitech, Kent, UK). The silver in this step played the role of catalyst for the etching chemistry. HF etching was carried out in a PTFE container in an etching solution with a volume ratio of Ethanol:HF(49%):H_2O_2(30%) = 1:1:1. The silver patterned microreactors were immersed into the etching solution and were etched for different time periods (e.g., 30 and 45 min). Afterwards, the microreactors were transferred into an ethanol bath for 30 min and then washed in a 30% HNO_3 solution for 30 min to remove the silver residue in the silicon. The microreactors were then rinsed thoroughly with DI water and dried under nitrogen stream.

2.1.2. Catalyst Deposition

The next stage of the process is the deposition of the silver catalyst on the porous silicon structure. Prior to its deposition, the microreactors were cleaned again using piranha solution. The same shadow mask used to define the porous silicon structure was used to define the catalytic reaction area by covering the reactor side walls. A layer of silver (equivalent to a thickness of 250 nm for flat geometry) was deposited onto the reaction channel by the sputter coater, which was operated with multi-time cycles, a procedure based on a prior calibration. The amount of silver deposited on the defined catalyst area was checked by weighing the silicon reactors before and after the sputter coating and was found to be ~2×10^{-4} g. This value was very close to that calculated based on the flat geometric area and the thickness of the silver layer (1.9×10^{-4} g).

2.1.3. Anodic Bonding

The silicon microreactor with the silver catalyst was then bonded with a glass wafer (Corning 7740; Corning, NY, USA) cleaned using piranha solution. The anodic bonding was carried out at 450 °C and 500–1000 V. The microreactors with porous silicon were named based on the HF etching time: Psi-Ag-30 for etching time of 30 min and Psi-Ag-45 for etching time of 45 min. Film-Ag was the microreactor with the flat non-porous silicon. The bonded microreactor with silver catalyst is shown in Figure 2b.

2.2. Characterization of Porous Silicon and Silver Catalyst

To characterize the pore structure of the porous silicon formed, flat silicon wafers were etched separately by HF solution following the procedure described above. The surface area was determined using N_2 adsorption-desorption isotherm (BET) measurement (Tristar 3000; Micromeritics Instrument Corporation, Norcross, GA, USA). In order to load the porous silicon sample into the glass measurement tube, the substrates were diced in pieces of 6 × 10 mm. The samples were degassed at 135°C in helium overnight before BET measurement. The surface morphology of the porous silicon was examined by SEM (Jeol JSM-6480LV; JEOL Ltd., Tokyo, Japan). The composition of the silver catalyst deposited on the porous silicon layer was also examined by SEM (Jeol JSM-6480LV; JEOL Ltd., Tokyo, Japan), using an Electron Backscattered Diffraction Detector (EBSD). An SEM (Jeol JSM-7401; JEOL Ltd., Tokyo, Japan) equipped with an upper secondary electron in-lens detector (SEI), a lower secondary electron detector (LEI), and a backscattered electron detector (BEI) was used for observation of the cross-section. For observation of the cross-section structure, the substrates were cleaved manually.

2.3. Experimental Set-Up and Procedure

The microreactor was first assembled with an inlet/outlet connector and a heating unit, as shown in Figure 3A. The inlet and outlet were sealed using O-rings (Perlast® G80A; O Rings Ltd., Chichester, UK) and a stainless steel housing/connector (Figure 3A). The microreactor was heated on both sides using two ceramic heaters (Ultramic™ 600; Watlow Ltd., Nottingham, UK), with a spacer made of 1.5 mm thick graphite sheet (Figure 3B). The assembled microreactor system, including a liquid evaporator, thermal insulation, a flow switching valve box and the line insulation is shown in Figure 3C. The schematic diagram of the setup is shown in Figure 4. A syringe pump (Cole Parmer 79400 series; Cole Parmer Instrument Co. Ltd., London, UK) was used to deliver the liquid alcohol to an evaporator where the vaporized alcohol was carried away by helium flow regulated by a mass flow controller. Oxygen was mixed with the alcohol-helium mixture at the outlet of the evaporator. At the outlet of the reactor, the reaction mixture was directed to a condenser/gas-liquid separator which was kept in an ice-water bath. The non-condensable gas was directed to a GC (Trace GC; ThermoQuest, Rodano, Italy) with Carboxen 1006 column and a thermal conductivity detector to determine the amount of CO_2 formed. Flow rate of the non-condensable gas was measured after the GC using a soap bubble flow meter. The liquid sample collected was analyzed using another GC (Agilent 6890; Agilent technologies Ltd., Cheshire, UK) with a HP-INNOWax column and a flame ionization detector. The

oxidation of rosalva on silver catalyst could lead to several other decenal isomers. Pure 9-decenal was not available but a mixture was obtained from Givaudan (90% decenal isomers, containing >50% of 9-decenal). Cis-4-decenal, cis-7-decenal and a mixture of decenal isomers all had a same GC retention time and same peak areas when their concentrations were the same. GC calibration for 9-decenal was carried out using cis-4-decenal as a standard. Identification of the aldehyde in reaction product was carried out using NMR analysis: ä$_H$ (500 MHz, $CDCl_3$) 1.23–1.42 (8H, m, 4× CH_2), 1.58–1.67 (2H, m, C^3H_2), 1.95–2.08 (2H, m, C^8H_2), 2.40 (2H, td, *J* 1.9 and 7.4, C^2H_2), 4.91 (1H, m, $C^{10}H_2$-*cis*), 4.94–5.02 (1H, m, $C^{10}H_2$-*trans*), 5.73–5.85 (1 H, m, C^9H), 9.74 (1 H, t, *J* 1.9, C^1HO); (Bruker 500 MHz; Bruker, Coventry, UK). The flow rate of the non-condensable gas was measured using a soap bubble meter. The carbon balance from the analysis was within ±3%.

The oxidation of rosalva was carried out under atmospheric pressure with oxygen as the oxidant and helium as the diluent gas. The residence time was calculated at reaction temperature. A blank test was carried out at 450 °C with a reaction mixture containing 1.75% rosalva and 17.5% oxygen with a residence time of 20 ms. Trace costenal was detected but was confirmed to be from the reactant rosalva. The activation of silver catalyst was carried out by repeated oxidation and reaction cycles at 450 °C. Oxygen was first passed through the microreactor for 1 h (oxidation) and then a standard inlet mixture (1.75% rosalva, 5.25% oxygen) for 1–2 h (reaction). The procedure was repeated until a stable activity (or the conversion of rosalva) was obtained. Between experiments (*i.e.*, overnight), the microreactor system was kept at 250 °C under a flow of 10% oxygen. A standard run was carried out each day at 450 °C and residence time 18 ms with the standard inlet mixture to check the catalyst activity. The reactor was replaced when the decrease in conversion in the standard run was larger than 10%.

Figure 3. Microreactor inserted in stainless steel housing/connector (**A**), ceramic heater system disassembled (**B**) and assembled microreactor-heater system (**C**).

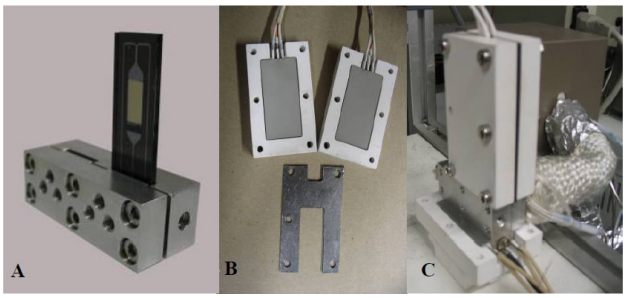

Figure 4. Experimental setup for the gas-phase oxidation of rosalva.

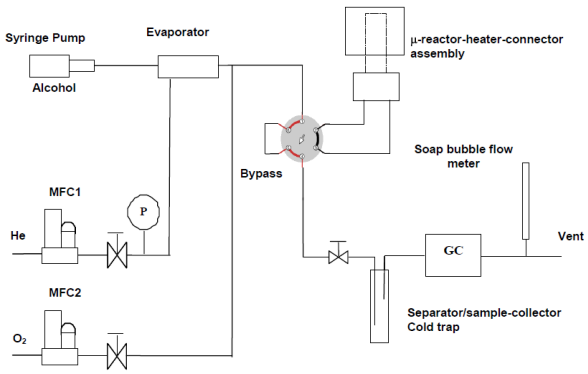

3. Results and Discussion

3.1. Characterisation of Porous Silicon and Silver Catalyst

The BET surface area was measured to be 0.30 and 0.38 m^2 g^{-1} for Psi-30 and Psi-45, respectively, and was based on the mass of the whole sample, including the porous and the solid layer. The actual porous areas were 0.023 and 0.029 m^2 for Psi-Ag-30 and Psi-Ag-45, respectively. The BET surface area measured in this work is comparable to those reported by Tiggelaar *et al.* [31] for porous silicon obtained by anodic oxidation, showing that the thicker the porous layer the larger the surface area.

SEM images of the top view of the porous silicon samples are shown in Figure 5. Both samples showed tortuous pores extending in the bulk of the Si wafer. Silver was deposited on the above samples with the procedure described in Section 2. The silver coated samples were treated in air at 450 °C. SEM images of the silver coated Psi-30 before and after heating treatment are shown in Figure 6. The silver coated porous surfaces look smoother, probably due to silver deposition covering/bridging small features of the porous silicon structure (Figure 6A). After thermal treatment, the silver coated porous surfaces do not show significant change (Figure 6B). Silver crystals with a diameter of ~1 μm are observed on top of the porous layer. The silver crystals and the silver on porous silicon were confirmed by SEM-EBSD analysis which gave a composition of 85% of Ag on the silver crystal and 65% of Ag on silver-porous silicon areas. Other elements detected were oxygen (11% on the silver crystal and 22% on silver-porous silicon area) and Si.

Figure 5. SEM images (top view) of porous silicon formed on n-type<100> silicon wafer etched in Ethanol/HF/H_2O_2 (volume ratio 1:1:1). (**A**) Psi-30 and (**B**) Psi-45.

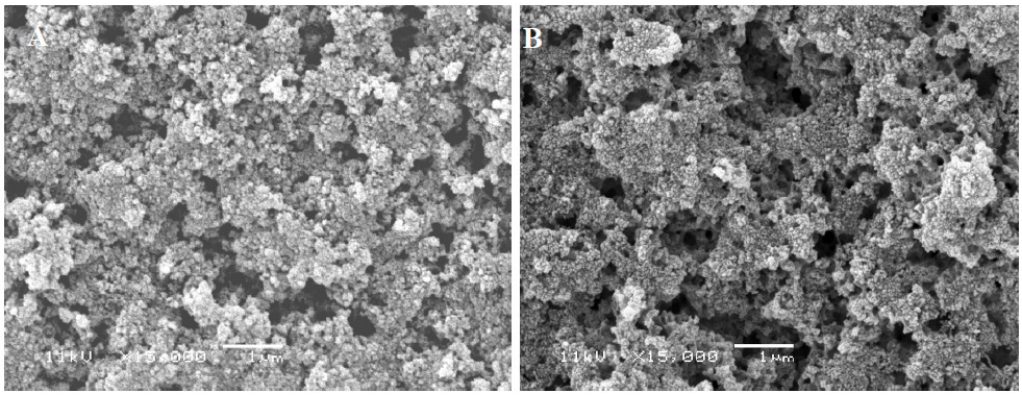

Figure 6. SEM images of Psi-Ag-30: (**A**) before and (**B**) after heating in an oven at 450 °C for 1 h.

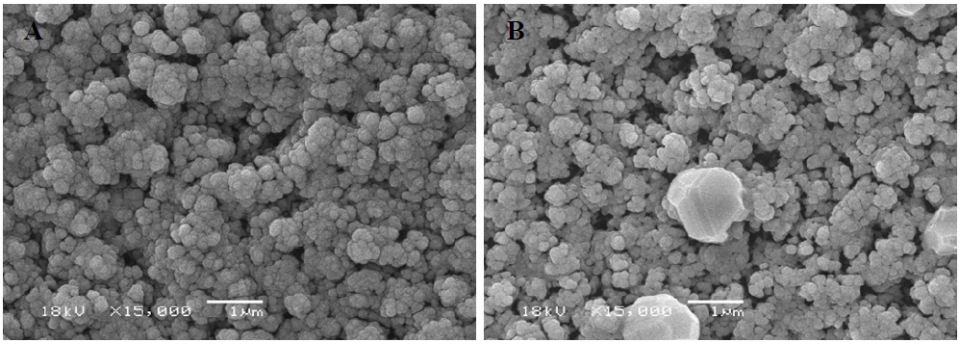

SEM images of the cross-section from SEM-LEI are shown in Figure 7. It can be seen from the top images of Figure 7A,B that the porosity of porous silicon along the depth of the layers is not uniform, with larger and more open pores on the upper part of the layer and smaller pores deeper in it. This leads to a porous silicon layer structure without a clear boundary between porous and solid silicon. However, the thickness of the porous silicon layer may be estimated to be 1–2 μm for Psi-30 and 2–3 μm for Psi-45, judged by the density of the porous structure, as seen in the top images in Figure 7. From the bottom images in Figure 7, which are obtained from SEM-COMPO analysis, the shining parts correspond to silver conformally coating the exposed cauliflower-like porous structure (Figure 6B). The scattered shining spots are silver particles which penetrated through the pores during sputter coating and deposited into a thin section beneath the conformal silver layer with particle sizes of 6–30 nm observed also by TEM (images not shown). On the contrary, flat silver films have been known to undergo restructuring upon heating and reaction; when a film is subjected to biaxial stress, local areas relax to different degrees generating a gradient between a relaxed grain and the surrounding film. Consequently, mass flow between the film and the substrate takes place. This results in the relaxed area growing out from the base as a hillock, which is more energetically favourable [32] and results in larger size particles. SEM images of thin Ag films on silicon before and after heat treatment show break-up of the granular film and agglomeration of some of the silver particles from a particle size of a few hundred nanometres to a few micrometers [33,34]. From our previous work on a thin Ag film catalyst, an average Ag particle size of ~1 μm after heat treatment was observed [30]. Thus, the porous structure stabilised the Ag coating and prevented agglomeration to a certain extent.

Figure 7. Side view SEM images of porous silicon supported silver: (**A**) Psi-Ag-30 and (**B**) Psi-Ag-45. Top: SEM-LEI, bottom: SEM-BEI.

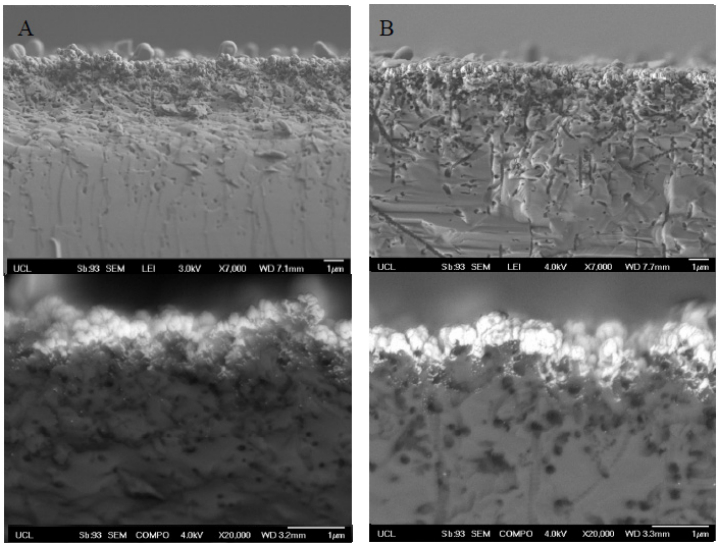

3.2. Rosalva Oxidation on Silver Catalyst

3.2.1. Effect of Reaction Temperature

The effect of reaction temperature on the oxidation of rosalva was first studied in the reactor Psi-Ag-30 over a temperature range of 375–475 °C with the standard inlet mixture (1.75% rosalva,

5.25% oxygen) at a residence time of 18 ms. To examine performance enhancement by using the porous silicon as catalyst support, the same experiment was also carried out in a microreactor with thin film silver catalyst. The main product of the reaction was 9-decenal which was confirmed by performing NMR analysis; total alternative aldehyde content was ~1%. CO and H_2 were not detected when the non-condensable gas was analysed using a third GC (Agilent, 7890; Agilent technologies Ltd., Cheshire, UK) with a molecular sieve column. Decenoic acid and CO_2 were the only side products detected. The results are presented in Table 1 showing the effect of temperature on the conversion of rosalva and the selectivity to costenal, 9-decenoic acid and CO_2. In the reactor Psi-Ag-30, the conversion of rosalva increases with temperature significantly, while the selectivity to costenal is less affected by reaction temperature and slightly decreases from 98.7%–96.2% with temperature increases from 375–475 °C. The selectivity to CO_2 and the acid together is about 2%–4% in the temperature range studied. The selectivity to CO_2 increases slightly with temperature which is just detectable at 375 °C and increases to ~2.5% at 475 °C; while the selectivity to the acid is less affected by the reaction temperature. In the reactor Film-Ag, the dependency of conversion and selectivity of the reaction on temperature is the same as those in Psi-Ag-30. However, the performance of the film silver catalyst is poorer than that of the silver supported on porous silicon. Conversions of rosalva are 7.7% at 425 °C and 35% at 475 °C compared to 66% and 91% obtained in Psi-Ag-30 at the same reaction temperatures.

Table 1. Conversion and selectivity at different reaction temperatures on two forms of silver catalyst: the porous silicon supported silver Psi-Ag-30 and the thin film silver catalyst Film-Ag (Inlet mixture: 1.75% rosalva, 5.25% oxygen with helium as balance; residence time: 18 ms).

T, °C	Psi-Ag-30				Film-Ag			
	X, %	Selectivity, %			X, %	Selectivity, %		
		9-decenal	9-decenoic acid	CO_2		9-decenal	9-decenoic acid	CO_2
375	23.3	98.7	1.3					
400	43.2	98.2	1.6	0.2				
425	66.3	97.6	1.7	0.7	7.7	100		
450	81.8	96.9	1.2	1.9	14.4	98.9		1.1
475	91.4	96.2	1.2	2.5	35.1	95.3	3.0	1.7

The enhanced performance of the oxidation of rosalva on the porous silicon supported silver catalyst is clearly demonstrated by the data in Table 1. Turnover frequencies (TOF) (based on moles of Ag) for the consumption of rosalva at 450 °C is calculated to be 225 h^{-1} on Psi-Ag-30 which is about 5.6 times higher than that on Film-Ag (40 h^{-1}). The enhancement could be attributed to the increase of catalyst surface area and different catalyst morphology. The rough porous structure (Figures 5 and 6) increased the dispersion of the silver catalyst and produced a conformal layer contrary to the silver deposited on flat silicon wafer surface [30]. Oxygen diffusion in silver occurs via both grain boundary and interstitial diffusion at temperatures below 900 K [35]. The importance of oxygen diffusion along grain boundaries and related structural faults for silver-catalysed oxidation reactions has been

demonstrated by Waterhouse *et al.* [36]. The catalyst surface morphology can also influence the state of the chemisorbed oxygen, which can have an impact on the reaction performance [35,37]. Restructuring of the catalyst surface also takes place with heating and reaction, and is dependent on a variety of factors, including temperature, partial pressure of oxygen and the initial morphology of the silver substrate.

The results can be compared with those reported by Gallezot *et al.* for the same reaction on 4.5 wt% Ag/SiC in a 75 cm^3 cylindrical Pyrex reactor [29]. The best results reported were 70% conversion of rosalva with selectivity to costenal of 73% at 450 °C at a contact time of 28 ms. Low selectivity to costenal in their work could be due to the experimental set-up, where total oxidation might take place in the gas phase or on the walls of vaporiser and in the reactor heated at 450 °C. Inefficient heat transfer in the catalyst bed giving rise to hot spots might also be a contribution to the total oxidation for such highly exothermic reaction. Hence, increasing reaction temperature above 450 °C might have caused an adverse effect on the selectivity because total oxidation was favoured [29]. In our work, the inertness of the microreactor was confirmed as there was no gas phase oxidation reaction detected during blank experiments. The low CO_2 selectivity and high selectivity to costenal observed here can be attributed to the highly isothermal behaviour of the microstructured reactor.

Figure 8. Dependence of conversion and selectivity on oxygen concentration. Reactor, Psi-Ag-30. Reaction temperature, 450 °C; inlet mixture, 1.75% rosalva, varying oxygen with helium as balance; residence time, 18 ms.

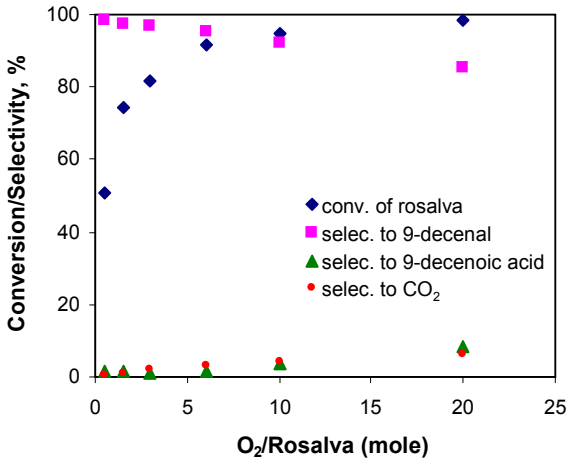

3.2.2. Effect of Inlet Oxygen Concentration

Effect of O_2 concentration on the reaction was studied at 450 °C with reactor Psi-Ag-30. The inlet rosalva concentration was kept at 1.75% while oxygen concentration was varied to adjust the ratio of O_2/rosalva from 0.5–20 with helium as balance. Residence time was kept at 18 ms. Results are shown in Figure 8. It can be seen that conversion of rosalva increases significantly with an increase in the ratio of O_2 to rosalva from 0.5–6. Further increasing O_2 leads to limited increase in conversion, as the reaction is close to completion. The selectivity to costenal decreases with the increase of O_2 concentration but not dramatically, from ~98%–~85% with the ratio of O_2/rosalva increasing from 0.5–20. The formation of 9-decenoic acid and CO_2 is favoured by increasing O_2 concentration, with selectivity to the acid and CO_2 of 8.6% and 6%, respectively, at an O_2/rosalva mole ratio of 20. The

increased formation of CO_2 could be due to total oxidation of the aldehyde with higher O_2 concentration [12]. It is worth noting that the selectivity to costenal was maintained at a relatively high value even at the ratio of O_2/rosalva of 20, while in a glass tube packed bed reactor an optimum ratio of 1.5 was observed [29].

3.2.3. Effect of Inlet Rosalva Concentration

Effect of rosalva concentration on the reaction was studied at 425 °C with reactor Psi-Ag-45. Rosalva concentration increased from 1.17%–3.43% while O_2 concentration was kept constant at 5.1%. The total inlet flow was balanced by helium and kept constant which produced a residence time of 18 ms. Results presented in Figure 9 show a decrease in conversion with increasing inlet rosalva concentration from 99.1%–79.2% in the range of concentrations studied. Selectivity to costenal increases slightly from 94.6%–96.8%. Selectivity to CO_2 was seen decreasing with the inlet rosalva concentration (4.2%–1.2%); selectivity to 9-decenoic acid was at ~1.2%–3.2%. It is noted that the ratio of O_2 to rosalva varied from 4.5–1.5 with the inlet concentration of rosalva changing from 1.17–3.41% due to the fixed O_2 inlet concentration (5.1%). The decrease in selectivity to CO_2 may also reflect the effect of the decreased O_2/rosalva ratio; the lower the O_2/rosalva ratio the less CO_2 formed by total oxidation. The average reaction rate on the silver catalyst increased with the inlet rosalva concentration (Figure 9) almost linearly. This might be an indication of a reaction order with respect to rosalva concentration close to one.

Figure 9. Dependence of conversion and selectivity on rosalva inlet concentration. Reactor, Psi-Ag-45. temperature, 425 °C; inlet mixture, 5.1% oxygen with helium as balance; residence time, 18 ms.

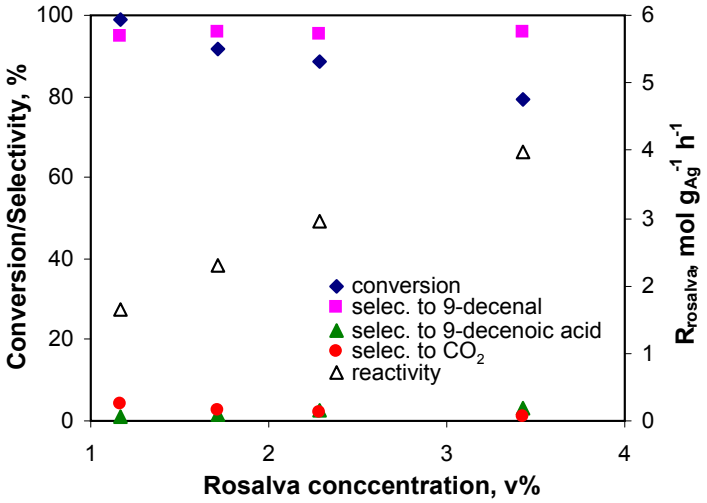

3.2.4. Effect of Residence Time

The effect of residence time was studied with the Psi-Ag-30 reactor at 450 °C by changing the total gas flow rate but keeping the concentration of the inlet mixture unchanged. The residence time varied from 0.009–0.027 s and the results are plotted in Figure 10. It can be seen that conversion of rosalva increases with residence time, having close to a first order dependence on rosalva concentration.

Selectivity is practically unaffected by residence time, changing from 97.3% at residence time of 9 ms to 96.5% at residence time of 27 ms. Selectivity to 9-decenoic acid and CO_2 was not significantly affected by the residence time and was at only 2.5%–3.5% in total.

Figure 10. Dependence of conversion and selectivity on residence time. Reactor, Psi-Ag-30; temperature, 450 °C; inlet mixture, 1.75% rosalva, 5.25% O_2 with helium as balance.

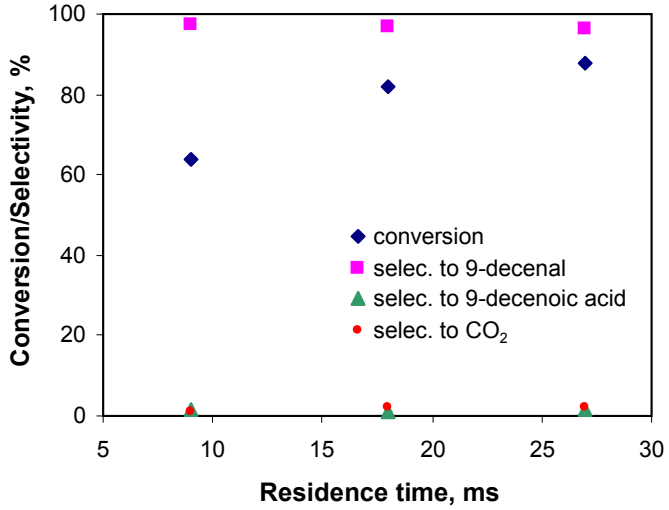

3.2.5. Effect of the Porous Silicon Layer Structure

Effect of the porous layer structure on the reaction was further examined by using the reactor Psi-Ag-45 which was etched longer in HF/H_2O_2 solution and had a thicker porous silicon layer and higher surface area. The reaction was carried out at a temperature range of 375–450 °C with the standard inlet mixture at a residence time of 18 ms. Results are plotted in Figure 11 together with the results from Psi-Ag-30 and Film-Ag for comparison. It can be seen from Figure 11 that the reaction showed higher conversion in Psi-Ag-45 than in Psi-Ag-30, with a conversion of 61% at 375 °C and close to complete (97% conversion) at 450 °C compared to 23% and 82% in Psi-Ag-30, respectively. Selectivity to costenal was not significantly affected by the reaction temperature in all three microreactors and was higher than 95% even at the highest reaction temperature (475 °C). The total selectivity to 9-decenoic acid and CO_2 was around 1%–5% in the same range of the reaction temperature. TOF for rosalva on Psi-Ag-45 at 450 °C is 268 h^{-1} compared to 225 h^{-1} on Psi-Ag-30 and 40 h^{-1} on Film-Ag.

To understand these results, a simple kinetic analysis was performed. For the standard inlet conditions (1.75% rosalva, 5.25% oxygen), the oxidation of rosalva on the porous silicon-supported silver shows approximately first order dependence on rosalva concentration (Figure 9). By assuming that the O_2 concentration was approximately constant during the reaction, which can be justified by the excess O_2 concentration in the inlet (ratio of O_2/rosalva of 3) and very low selectivity to CO_2, the reaction rate constants are estimated with a plug-flow reactor model from the data in Figure 11. An Arrhenius analysis was performed and the results are plotted in Figure 12. The activation energy is estimated to be 75.6, 77.3 and 130 kJ mol^{-1} for the reactions on Psi-Ag-30, Psi-Ag-45 and Film-Ag,

respectively. The activation energy on the film catalyst is almost double to these on the porous-supported silver.

Figure 11. Effect of porous structure on reaction performance (Inlet mixture: 1.75% rosalva, 5.25% oxygen with helium as balance; residence time: 18 ms).

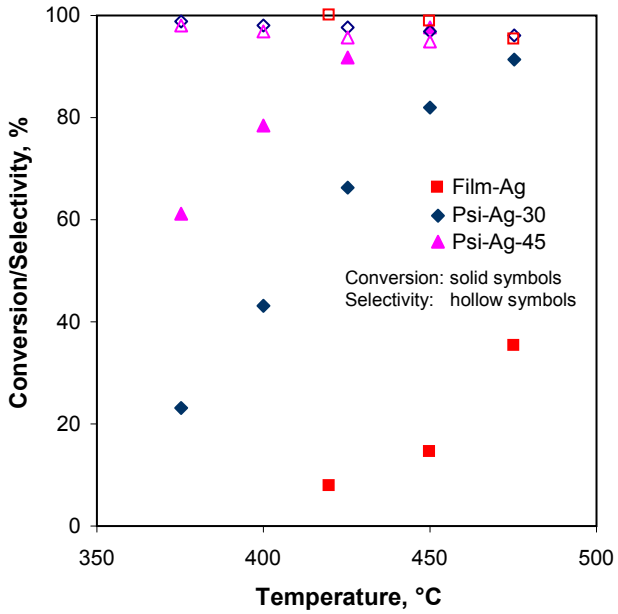

Figure 12. Arrhenius plot from data of Figure 10.

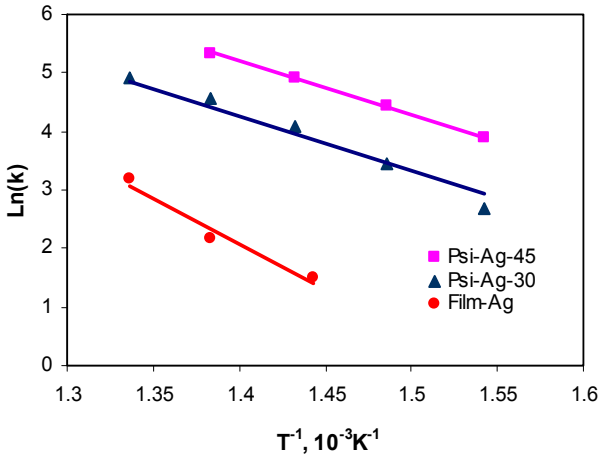

The activation energy values obtained in the three microreactors are within the range of typical catalytic reactions. However, a reduction in apparent activation energy for the porous silicon-supported catalysts, as compared to the flat silicon catalyst, may suggest the existence of mass transfer resistance for the former. In order to check for diffusion limitations in the porous layer, the Thiele modulus (φ) was calculated based on a first order reaction assumption:

$$\varphi = d\sqrt{\frac{k}{D_{eff}}}$$

where d is the thickness of porous layer, k is the reaction rate constant, D_{eff} is the effective diffusivity. The diffusivity of rosalva in air was estimated using Fuller's correlation [38]. The effective diffusivity was then approximated by one 10th of the bulk diffusivity. For the reaction in Psi-Ag-45 at 450 °C, k and D_{eff} were estimated to be 207 s^{-1} and 3×10^{-6} m^2 s^{-1}, respectively. With a thickness of the porous silicon layer of 3×10^{-6} m, φ was estimated to be 0.009, indicating absence of diffusion limitation.

Particle size and shape can significantly influence catalyst performance for structure sensitive reactions [39]. Nanoparticles with different sizes and shapes have different surface properties that can affect both selectivity and reactivity for various catalytic reactions. Such size effects are often observed in the size range of ~1–10 nm [40,41]. This particle size effect is unlikely in our work since most of the silver seems to be in the form of a conformal layer, while small particles would sinter at the high reaction temperature used. On the other hand, the physical and chemical properties of the flat silicon and the porous silicon surfaces could be different. As the porous silicon is formed in an HF solution, the exposed surface becomes terminated with hydrogen atoms and will typically oxidize in air at room temperature producing different types of surface species (Si-H, Si-O_x) [42,43]. Furthermore, porous silicon has a significantly different morphology as compared to flat silicon. These characteristics may result in different morphology, surface facets, electronic properties, non-equilibrium surface structures and metal-support interactions of the deposited catalytic layer/ particles, which have been shown to affect catalyst (and, in particular, Ag) reactivity [36,44–47].

4. Conclusions

The application of metal-assisted HF chemical etching as a simple method of producing porous structures in silicon microreactor channels has been demonstrated. The oxidation of rosalva to its aldehyde (costenal) on silver catalyst was successfully performed in silicon/glass microstructured reactors at temperatures of 375–475 °C. Significant performance enhancement was achieved by the porous silicon in the reaction channel, which increased the catalytic surface area. TOF for the rosalva consumption on the porous silicon supported silver was *ca.* six times that of flat silicon at 450 °C. Different activation energies were found for the porous silicon supported silver and for the thin film silver which could be due to different properties of the silver catalyst induced by the different chemical and physical properties of the support. Isothermal conditions in the microreactors allowed high conversions and selectivities to be achieved in a wide range of temperatures and oxygen concentrations. A selectivity of 95% even at 97% conversion levels was achieved in this work, which is higher than those reported in the literature for conventional laboratory packed bed reactors.

Acknowledgments

Financial support from EPSRC is gratefully acknowledged. We thank Chris Newman from Givaudan for supplying the costenal sample.

Conflicts of Interest

The authors declare no conflict of interest.

References

1. Sheldon, R.A.; van Bekkum, H. *Fine Chemicals through Heterogeneous Catalysis*; WILEY-VCH: Weinhein, Germany, 2001.
2. Della Pina, C.; Falletta, E.; Prati, L.; Rossi, M. Selective oxidation using gold. *Chem. Soc. Rev.* **2008**, *37*, 2077–2095.
3. Mallat, T.; Baiker, A. Oxidation of alcohols with molecular oxygen on solid catalysts. *Chem. Rev.* **2004**, *104*, 3037–3058.
4. Biella, S.; Rossi, M. Gas phase oxidation of alcohols to aldehydes or ketones catalysed by supported gold. *Chem. Commun.* **2003**, *9*, 378–379.
5. Han, D.; Xu, T.; Su, J.; Xu, X.; Ding, Y. Gas-Phase selective oxidation of benzyl alcohol to benzaldehyde with molecular oxygen over unsupported nanoporous gold. *ChemCatChem* **2010**, *2*, 383–386.
6. Della Pina, C.; Falletta, E.; Rossi, M. Highly selective oxidation of benzyl alcohol to benzaldehyde catalyzed by bimetallic gold-copper catalyst. *J. Catal.* **2008**, *260*, 384–386.
7. Shen, J.; Shan, W.; Zhang, Y.; Du, J.; Xu, H.; Fan, K.; Shen, W.; Tang, Y. Gas-phase selective oxidation of alcohols: In situ electrolytic nano-silver/zeolite film/copper grid catalyst. *J. Catal.* **2006**, *237*, 94–101.
8. Yadav, G.D.; Mewada, R.K. Selectivity engineering in the synthesis of value added chemicals: Oxidation of 1-octanol to 1-octanal over nano-fibrous Ag-OMS-2 catalysts. *Chem. Eng. Res. Des.* **2012**, *90*, 86–97.
9. Yamamoto, R.; Sawayama, Y.S.; Shibahara, H.; Ichihashi, Y.; Nishiyama, S.; Tsuruya, S. Promoted partial oxidation activity of supported Ag catalysts in the gas-phase catalytic oxidation of benzyl alcohol. *J. Catal.* **2005**, *234*, 308–317.
10. Hoelderich, W.F.; Kollmer, F. Oxidation reactions in the synthesis of fine and intermediate chemicals using environmentally benign oxidants and the right reactor system. *Pure Appl. Chem.* **2000**, *72*, 1273–1287.
11. Hessel, V.; Hardt, S.; Löwe, H. *Chemical Micro Process Engineering*. Weiley-VCH: Weinheim, Germany, 2004.
12. Cao, E.; Gavriilidis, A.; Motherwell, W.B. Oxidative dehydrogenation of 3-methyl-2-buten-1-o1 in microreactors. *Chem. Eng. Sci.* **2004**, *59*, 4803–4808.
13. Haas-Santo, K.; Fichtner, M.; Schubert, K. Preparation of microstructure compatible porous supports by sol-gel synthesis for catalyst coatings. *Appl. Catal. A* **2001**, *220*, 79–92.
14. Meille, V. Review on methods to deposit catalysts on structured surfaces. *Appl. Catal. A* **2006**, *315*, 1–17.
15. Losey, M.W.; Jackman, R.J.; Firebaugh, S.L.; Schmidt, M.A.; Jensen, K.F. Design and fabrication of microfluidic devices for multiphase mixing and reaction. *J. Microelectromech. Syst.* **2002**, *11*, 709–717.
16. Schilke, K.F.; Wilson, K.L.; Cantrell, T.; Corti, G.; McIlroy, D.N.; Kelly, C. A novel enzymatic microreactor with aspergillus oryzae β-galactosidase immobilized on silicon dioxide nanosprings. *Biotechnol. Prog.* **2010**, *26*, 1597–1605.

17. Huang, Z.; Geyer, N.; Werner, P.; de Boor, J.; Gösele, U. Metal-assisted chemical etching of silicon: A review. *Adv. Mater.* **2011**, *23*, 285–308.
18. Drott, J.; Lindström, K.; Rosengren, L.; Laurell, T. Porous silicon as the carrier matrix in microstructured enzyme reactors yielding high enzyme activities. *J. Micromech. Microengineer.* **1997**, *7*, 14–23.
19. Stewart, M.P.; Buriak, J.M. Chemical and biological applications of porous silicon technology. *Adv. Mater.* **2000**, *12*, 859–869.
20. Pichonat, T.; Gauthier-Manuel, B. A new process for the manufacturing of reproducible mesoporous silicon membranes. *J. Membrane Sci.* **2006**, *280*, 494–500.
21. Clicq, D.; Tjerkstra, R.W.; Gardeniers, J.G.E.; van den Berg, A.; Baron, G.V.; Desmet, G. Porous silicon as a stationary phase for shear-driven chromatography. *J. Chromatogr. A* **2004**, *1032*, 185–191.
22. De Malsche, W.; Clicq, D.; Verdoold, V.; Gzil, P.; Desmet, G.; Gardeniers, H. Integration of porous layers in ordered pillar arrays for liquid chromatography. *Lab Chip* **2007**, *7*, 1705–1711.
23. Li, X.; Bonn, P.W. Metal-assisted chemical etching in HF/H_2O_2 produces porous silicon. *Appl. Phys. Lett.* **2000**, *77*, 2572–2574.
24. Chern, W.; Hsu, K.; Chun, I.; Azeredo, B.; Fang, N.; Ferreira, P.; Li, X. Non-lithographic patterning and metal-assisted chemical etching for manufacturing of tunable light-emitting silicon nanowire arrays. In Proceedings of Lasers and Electro-Optics/Quantum Electronics and Laser Science Conference: 2010 Laser Science to Photonic Applications, San Jose, CA, USA, 16–21 May 2010; IEEE: Piscataway, NJ, USA, 2010.
25. Banwell, M.G.; McRae, K.J. Chemoenzymatic synthesis of (+)-aspicilin from chlorobenzene. *Org. Lett.* **2000**, *2*, 3583–3586.
26. Bortolini, O.; Campestrini, S.; di Furia, F.; Modena, G.; Valle, G. Metal catalysis in oxidation by peroxides. Anionic molybdenum-picolinate *N*-oxido-peroxo complex: An effective oxidant of primary and secondary alcohols in nonpolar solvents. *J. Org. Chem.* **1987**, *52*, 5467–5469.
27. McErlean, C.S.P.; Proisy, N.; Davis, C.J.; Boland, N.A.; Sharp, S.Y.; Boxall, K.; Slawin, A.M.Z.; Workman, P.; Moody, C.J. Synthetic ansamycins prepared by a ring-expanding Claisen rearrangement. Synthesis and biological evaluation of ring and conformational analogues of the Hsp90 molecular chaperone inhibitor geldanamycin. *Org. Biomol. Chem.* **2007**, *5*, 531–546.
28. Uyanik, M.; Akakura, M.; Ishihara, K. 2-iodoxybenzenesulfonic acid as an extremely active catalyst for the selective oxidation of alcohols to aldehydes, ketones, carboxylic acids, and enones with oxone. *J. Amer. Chem. Soc.* **2009**, *131*, 251–262.
29. Gallezot, P.; Ceroni, L.; Perrard, A. Oxidative dehydrogenation of rosalva to costenal on supported silver catalysts. *J. Mol. Catal. A* **1998**, *129*, L127–L130.
30. Cao, E.; Gavriilidis, A. Oxidative dehydrogenation of methanol in a microstructured reactor. *Catal. Today* **2005**, *110*, 154–163.
31. Tiggelaar, R.M.; Verdoold, V.; Eghbali, H.; Desmet, G.; Gardeniers, J.G.E. Characterization of porous silicon integrated in liquid chromatography chips. *Lab Chip* **2009**, *9*, 456–463.
32. Chaudhari, P. Hillock growth in thin films. *J. Appl. Phys.* **1974**, *45*, 4339–4346.
33. Sharma, S.K.; Spitz, J. Hillock growth and agglomeration in thin silver films. *Thin Solid Films* **1979**, *61*, L13–L15.

34. Sharma, S.K.; Spitz, J. Hillock formation, hole growth and agglomeration in thin silver films. *Thin Solid Films* **1980**, *65*, 339–350.
35. Waterhouse, G.I.N.; Bowmaker, G.A.; Metson, J.B. Oxygen chemisorption on an electrolytic silver catalyst: A combined TPD and Raman spectroscopic study. *Appl. Surface Sci.* **2003**, *214*, 36–51.
36. Waterhouse, G.I.N.; Bowmaker, G.A.; Metson, J.B. Influence of catalyst morphology on the performance of electrolytic silver catalysts for the partial oxidation of methanol to formaldehyde. *Appl. Catal. A* **2004**, *266*, 257–273.
37. Waterhouse, G.I.N.; Bowmaker, G.A.; Metson, J.B. Mechanism and active sites for the partial oxidation of methanol to formaldehyde over an electrolytic silver catalyst. *Appl. Catal. A* **2004**, *265*, 85–101.
38. Hayes, R.E.; Kolaczkowski, S.T. *Introduction to Catalytic Combustion*; Gordon & Breach Science Publishers: Amsterdam, The Netherlands, 1997.
39. van Santen, P.A.; Neurock, M. *Molecular Heterogeneous Catalysis-A Conceptual and Computational Approach*; WILEY-VCH: Weinheim, Germany, 2006.
40. Che, M.; Bennett, C.O. The influence of particle size on the catalytic properties of supported metals. In *Advances in Catalysis*; H.P.D.D., Eley, Paul, B.W., Eds.; Academic Press: New York, NY, USA, 1989; Volume 36, pp. 55–172.
41. Musselwhite, N.; Somorjai, G. Investigations of structure sensitivity in heterogeneous catalysis: from single crystals to monodisperse nanoparticles. *Top. Catal.* **2013**, *56*, 1277–1283.
42. Anderson, R.C.; Muller, R.S.; Tobias, C.W. Chemical surface modification of porous silicon. *J. Electrochem. Soc.* **1993**, *140*, 1393–1396.
43. Michael, J.S. *Porous silicon in Practice: Preparation, Characterization and Applications*, First ed.; Wiley-VCH: Weinheim, Germany, 2012.
44. Tsybulya, S.V.; Kryukova, G.N.; Goncharova, S.N.; Shmakov, A.N.; Balzhinimaev, B.S. Study of the real structure of silver supported catalysts of different dispersity. *J. Catal.* **1995**, *154*, 194–200.
45. Mastikhin, V.M.; Goncharova, S.N.; Tapilin, V.M.; Terskikh, V.V.; Balzhinimaev, B.S. Effect of particle size upon catalytic and electronic properties of supported Ag catalysts: Combined catalytic, 109Ag NMR and quantum chemistry studies. *J. Mol. Catal. A* **1995**, *96*, 175–179.
46. Zuburtikudis, I.; Saltsburg, H. Linear metal nanostructures and size effects of supported metal catalysts. *Science* **1992**, *258*, 1337–1339.
47. Christopher, P.; Linic, S. Shape- and size-specific chemistry of Ag nanostructures in catalytic ethylene epoxidation. *ChemCatChem* **2010**, *2*, 78–83.